

**Electronic Supplementary Information**

Enhanced Thermal Conductivity of Nanocomposites with MOF-derived Encapsulated  
Magnetic Oriented Carbon Nanotube-Grafted Graphene Polyhedra

Xu Li,<sup>a</sup> Ya Li,<sup>a</sup> Md Mofasserul Alam,<sup>b</sup> Peng Chen,<sup>a</sup> Ru Xia,<sup>a</sup> Bin Wu,<sup>\*a</sup> Jiasheng Qian<sup>\*a</sup>

<sup>a</sup> Key Laboratory of Environment-Friendly Polymeric Materials of Anhui Province,  
School of Chemistry & Chemical Engineering, Anhui University, Hefei, 230601, China

<sup>b</sup> CAS Key Laboratory of Soft Matter Chemistry, Collaborative Innovation Centre of  
Chemistry for Energy Materials, School of Chemistry and Materials Science,  
University of Science and Technology of China, Hefei, 230026, China

\*Corresponding Author

E-mail address: lwbin@ahu.edu.cn (B Wu), qianjsh@ahu.edu.cn (J. S. Qian).

**Content:**

**Fig. S1** Schematic illustrations of the preparation process of Co@Co<sub>3</sub>O<sub>4</sub>-G.

**Table. S1** Physical properties of ER/Co@Co<sub>3</sub>O<sub>4</sub>-G nanocomposites with different Co@Co<sub>3</sub>O<sub>4</sub>-G volume fractions.

**Fig. S2** The XRD of ZIF-67.

**Fig. S3** Images of Co@Co<sub>3</sub>O<sub>4</sub>-G dispersion in a water solution (a) and its response to external magnetic field when a magnet is placed near the dispersion (b).

**Fig. S4** Full survey XPS of Co-N/C (a) and Co@Co<sub>3</sub>O<sub>4</sub>-G(b), N 1s of Co-N/C (c) and Co@Co<sub>3</sub>O<sub>4</sub>-G (d).

**Fig. S5** SEM image of ZIF-67.

**Fig. S6** (a) TEM of Co@Co<sub>3</sub>O<sub>4</sub>-G. (b) TEM-EDS elemental mapping of O atom in Co@Co<sub>3</sub>O<sub>4</sub>-G. (c) The corresponding EDS spectrum of Co@Co<sub>3</sub>O<sub>4</sub>-G. (d) The weight and atoms percentage of C, Co, O and N in the Co@Co<sub>3</sub>O<sub>4</sub>-G.

**Fig. S7** The HRTEM of ultra-thin section of ER/Co@Co<sub>3</sub>O<sub>4</sub>-G with 8.7 vol% loading of Co@Co<sub>3</sub>O<sub>4</sub>-G.

**Fig. S8** The atomic vibrogram of G $\cap$ CNT with time in EMD simulate.

**Fig. S9** The change of HCACF of the G $\cap$ CNT and the junction with time.

**Fig.S10** The thermal conductivity with 8.7 vol% with the change of magnetic field intensity

**Fig. S11** Thermal conductivity of the ER/Co@Co<sub>3</sub>O<sub>4</sub>-G nanocomposites with different loading and other CNT based composites reported in previous work.

**Fig. S12** Thermal conductivity of the ER/Co@Co<sub>3</sub>O<sub>4</sub>-G nanocomposites with different loading and other CNT and graphene-based composites reported in previous work.

**Fig. S13** The thermal conductive mechanism of G $\cap$ CNT.

**Fig. S14** Frequency dependence of electric conductivity of the nanocomposites with different loading.

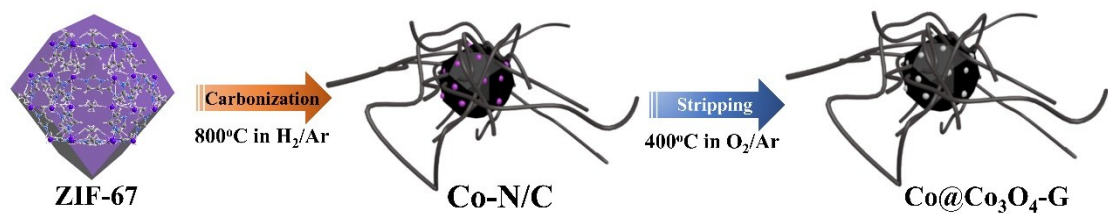


**Fig. S1** Schematic illustrations of the preparation process of  $\text{Co}@\text{Co}_3\text{O}_4$ -G.

**Table. S1** Physical properties of ER/Co@Co<sub>3</sub>O<sub>4</sub>-G nanocomposites with different Co@Co<sub>3</sub>O<sub>4</sub>-G volume fractions.

Vol. fraction (Vol%)	Density (g cm <sup>-3</sup> )	Specific heat capacity (J g <sup>-1</sup> K <sup>-1</sup> )	Thermal diffusivity (mm <sup>2</sup> s <sup>-1</sup> )	Thermal conductivity (W m <sup>-1</sup> K <sup>-1</sup> )
0	1.05	1.38	0.13	0.19
	1.02	1.34	0.12	0.17
	1.08	1.36	0.15	0.22
1.2	1.23	1.31	0.19	0.32
	1.19	1.33	0.22	0.35
	1.22	1.28	0.17	0.27
2.6	1.24	1.32	0.34	0.56
	1.26	1.31	0.36	0.60
	1.27	1.30	0.29	0.48
4.3	1.28	1.29	0.80	1.32
	1.29	1.28	0.83	1.37
	1.27	1.26	0.79	1.27
6.5	1.32	1.22	1.04	1.67
	1.35	1.23	1.03	1.72
	1.37	1.25	0.91	1.56
8.7	1.38	1.21	1.26	2.11
	1.37	1.18	1.39	2.24
	1.37	1.16	1.30	2.07

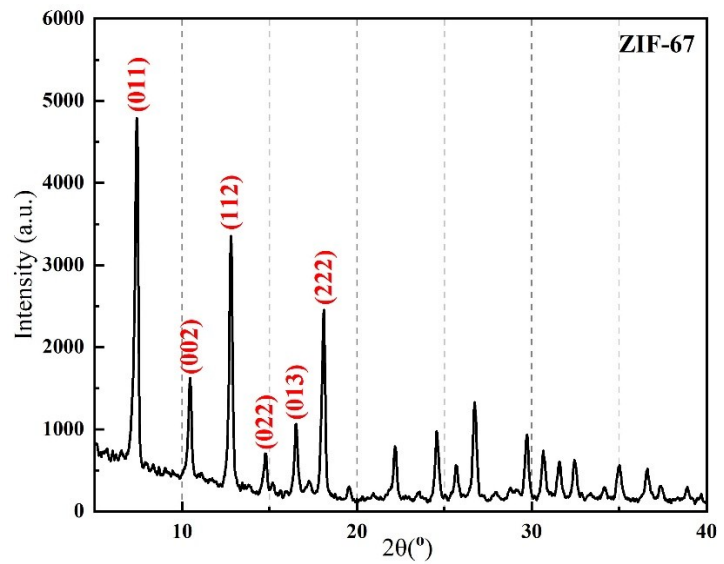


**Fig. S2** The XRD of ZIF-67.

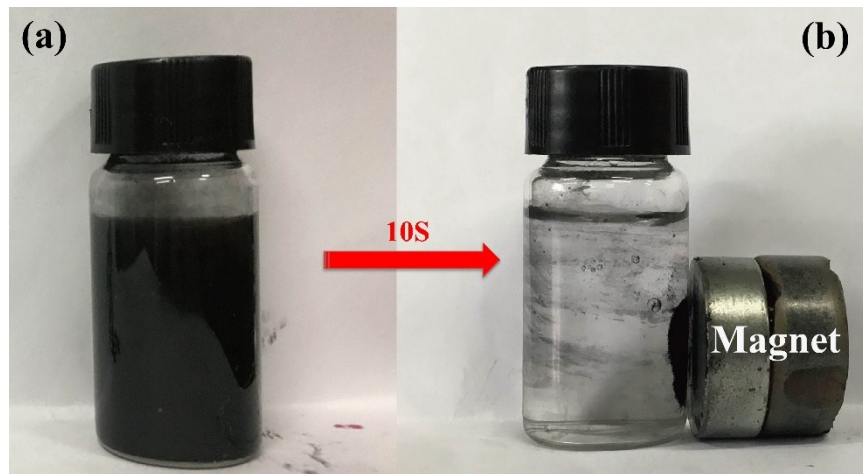


**Fig. S3** Images of Co@Co<sub>3</sub>O<sub>4</sub>-G dispersion in a water solution (a) and its response to external magnetic field when a magnet is placed near the dispersion (b).

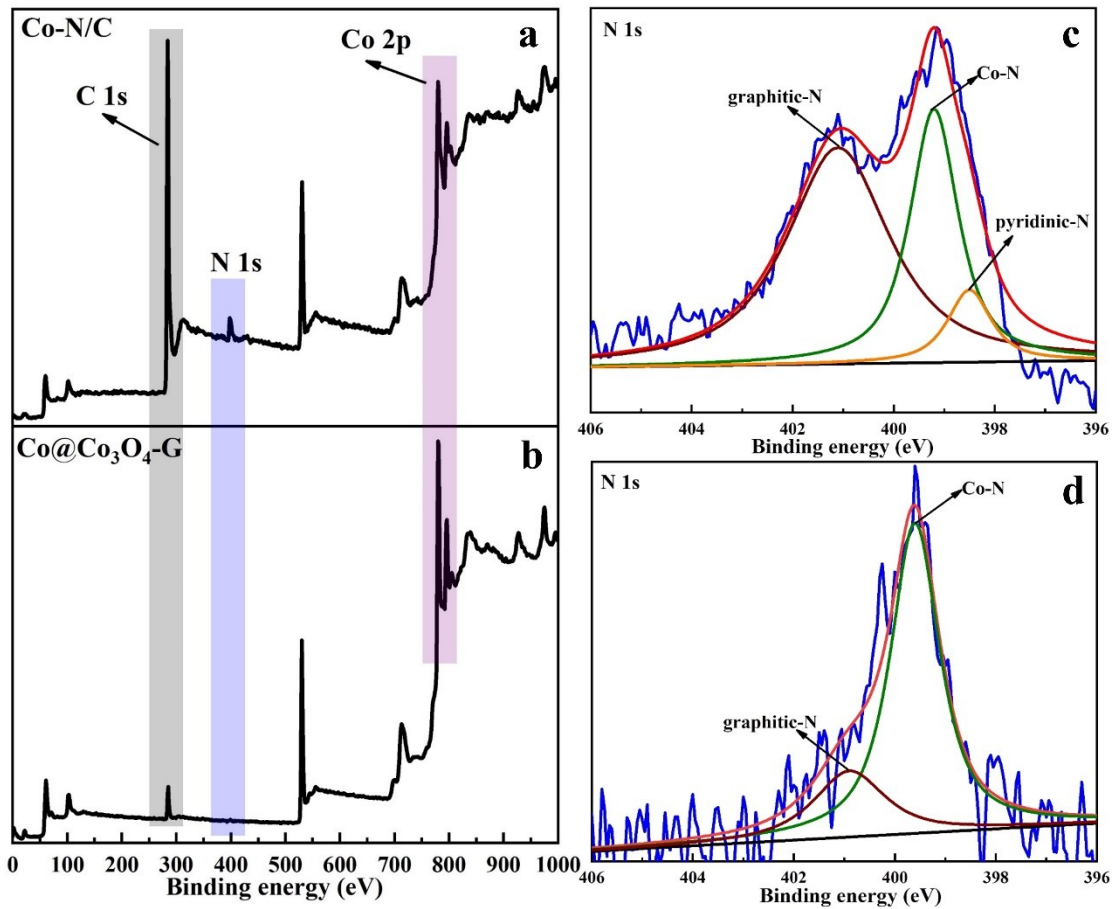


**Fig. S4** Full survey XPS of Co-N/C (a) and Co@Co<sub>3</sub>O<sub>4</sub>-G(b), N 1s of Co-N/C (c) and Co@Co<sub>3</sub>O<sub>4</sub>-G(d).

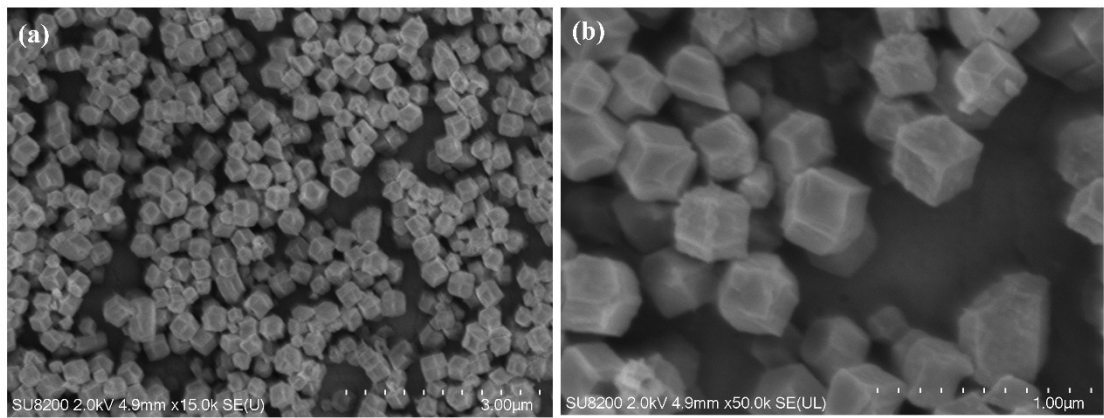


**Fig. S5** SEM image of ZIF-67.

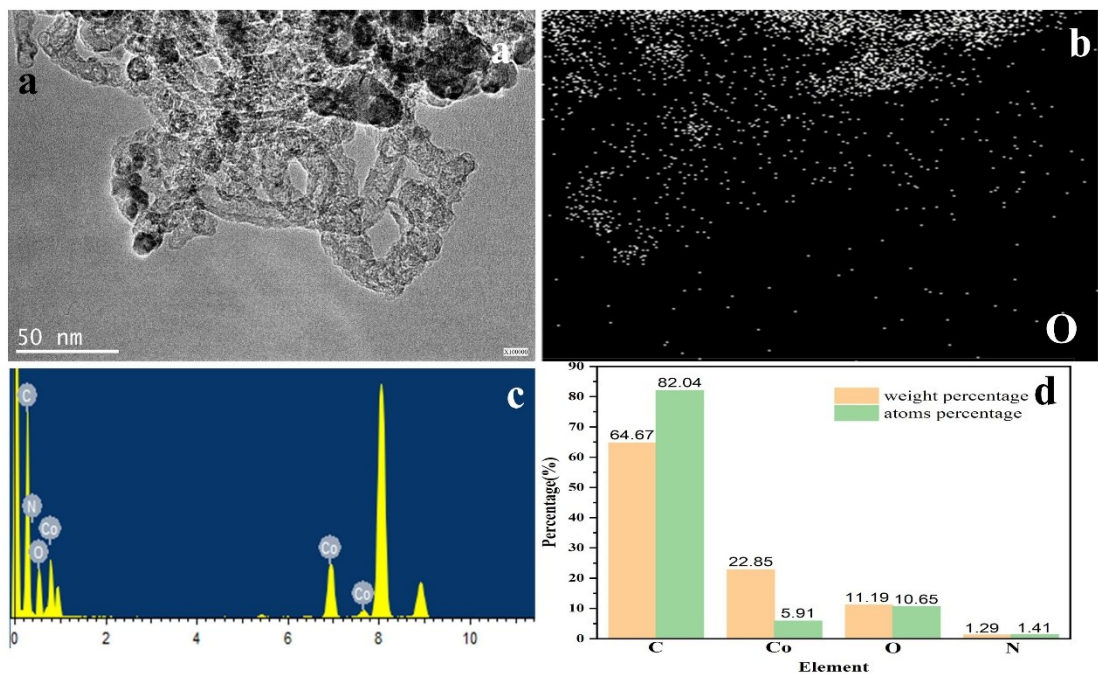


**Fig. S6** (a) TEM of Co@Co<sub>3</sub>O<sub>4</sub>-G. (b) TEM-EDS elemental mapping of O atom in Co@Co<sub>3</sub>O<sub>4</sub>-G. (c) The corresponding EDS spectrum of Co@Co<sub>3</sub>O<sub>4</sub>-G. (d) The weight and atoms percentage of C, Co, O and N in the Co@Co<sub>3</sub>O<sub>4</sub>-G.

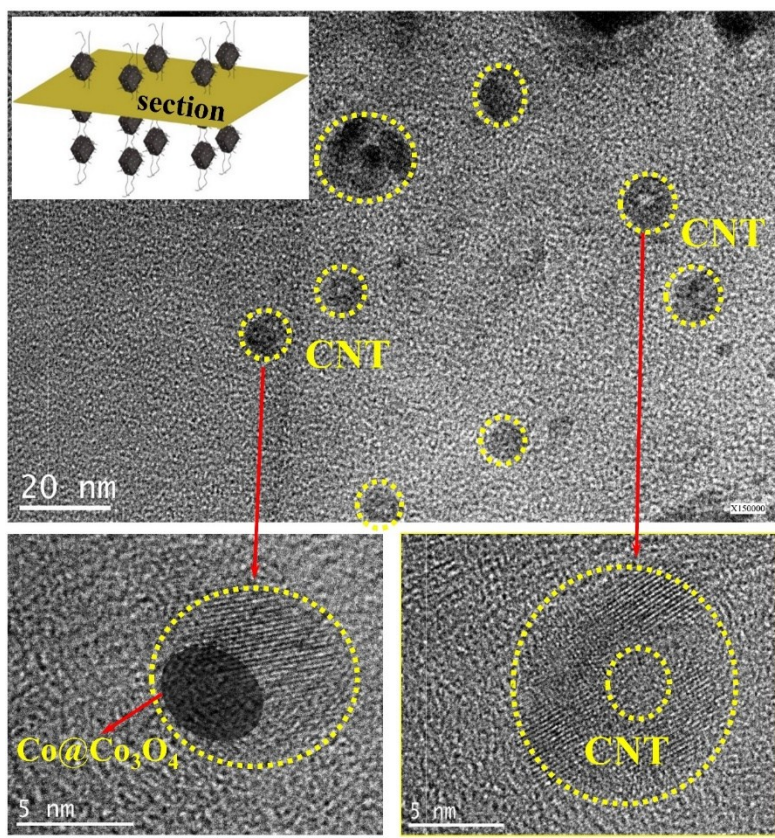


**Fig. S7** The HRTEM of ultra-thin section of ER/Co@Co<sub>3</sub>O<sub>4</sub>-G with 8.7 vol% loading of Co@Co<sub>3</sub>O<sub>4</sub>-G.

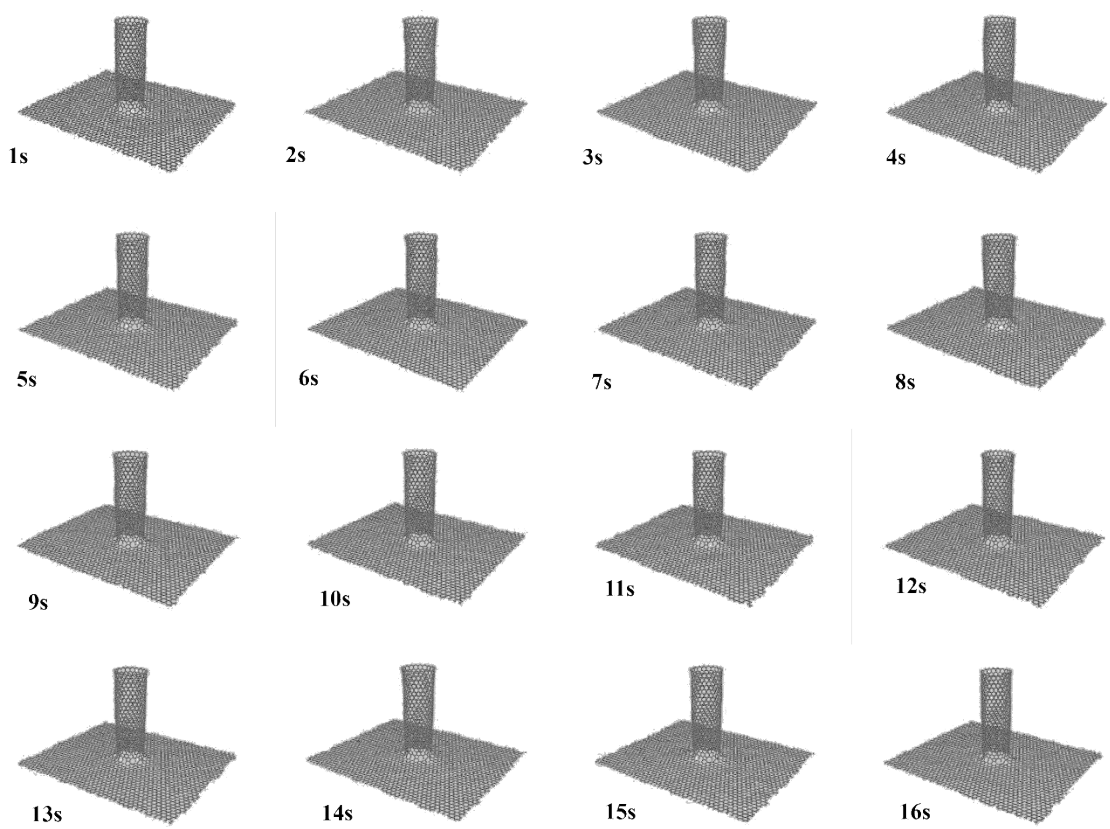


**Fig. S8** the atomic vibrogram of  $G \cap CNT$  with time in EMD simulate.

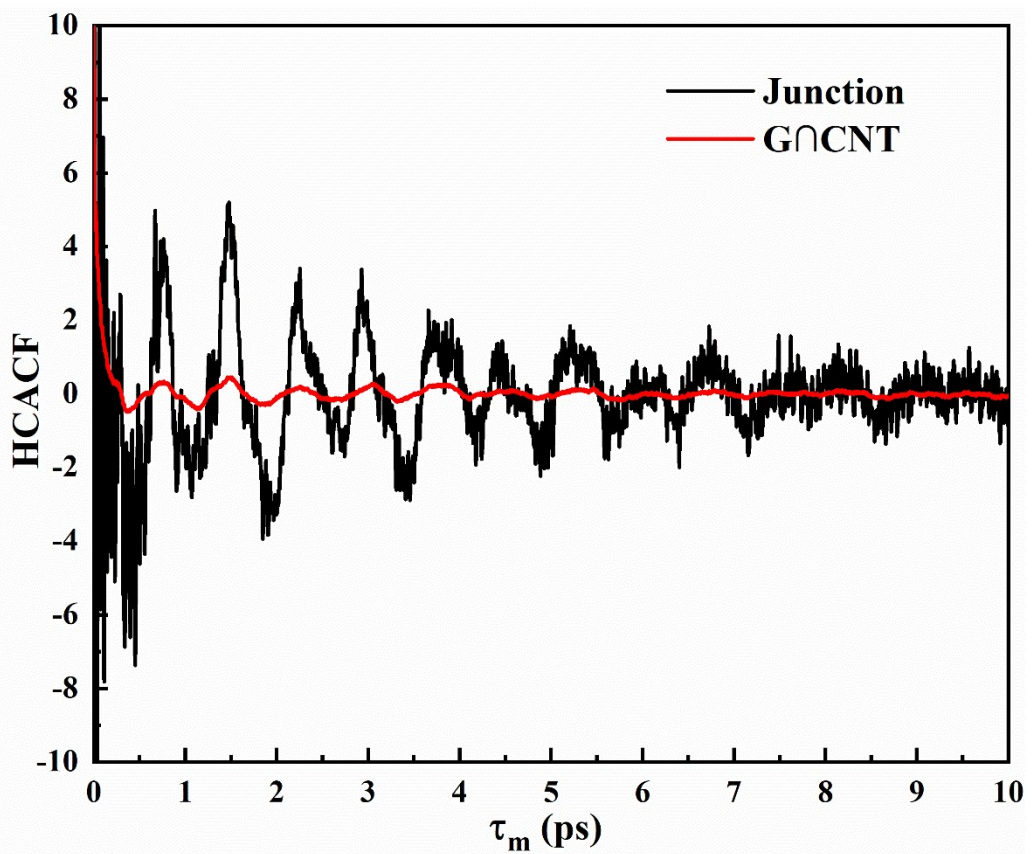


**Fig. S9** The change of HCACF of the  $G \cap CNT$  and the junction with time.

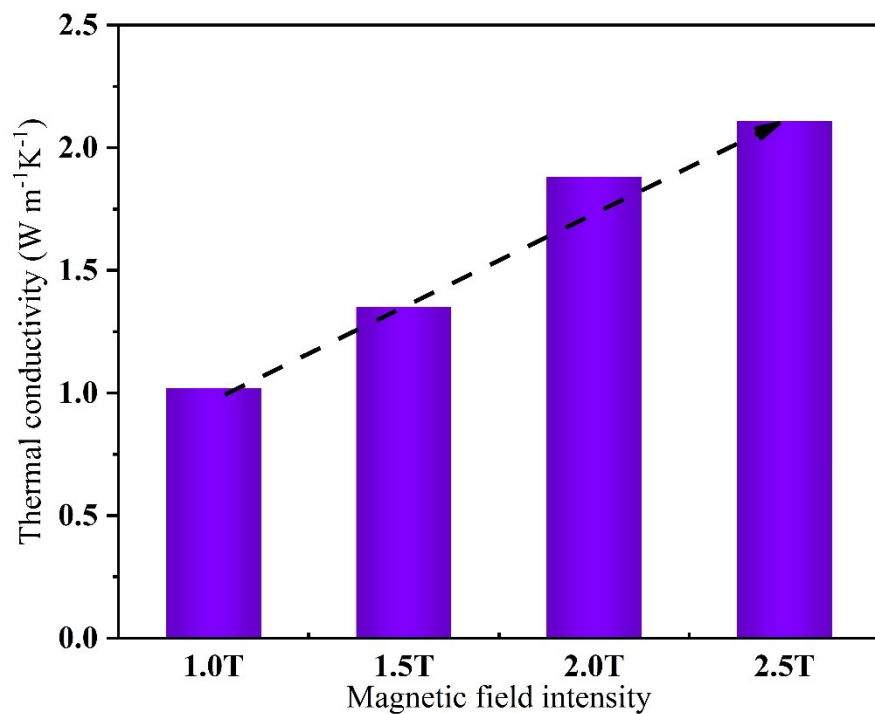


**Fig. S10** The thermal conductivity of nanocomposites with 8.7 vol% loading with the change of magnetic field intensity

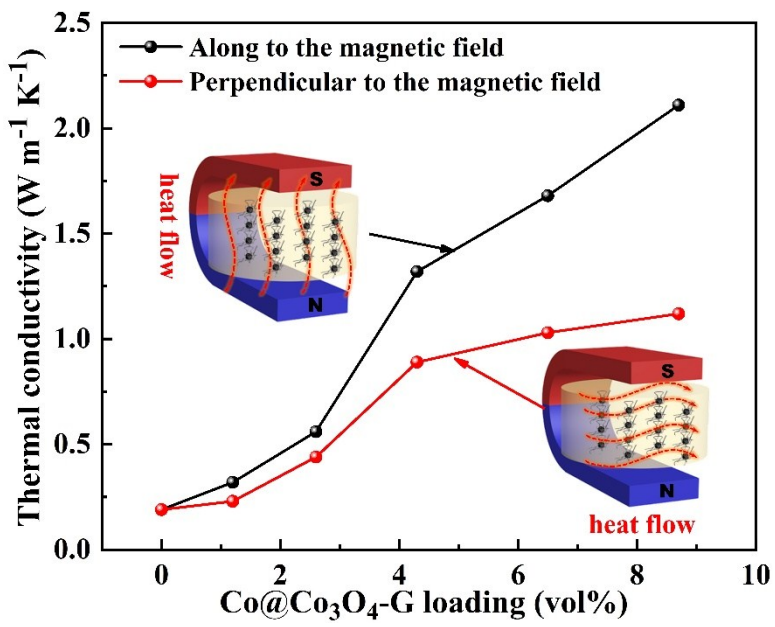


**Fig. S11** the thermal conductivity of ER/Co@Co<sub>3</sub>O<sub>4</sub>-G with different loading along different heat flow.

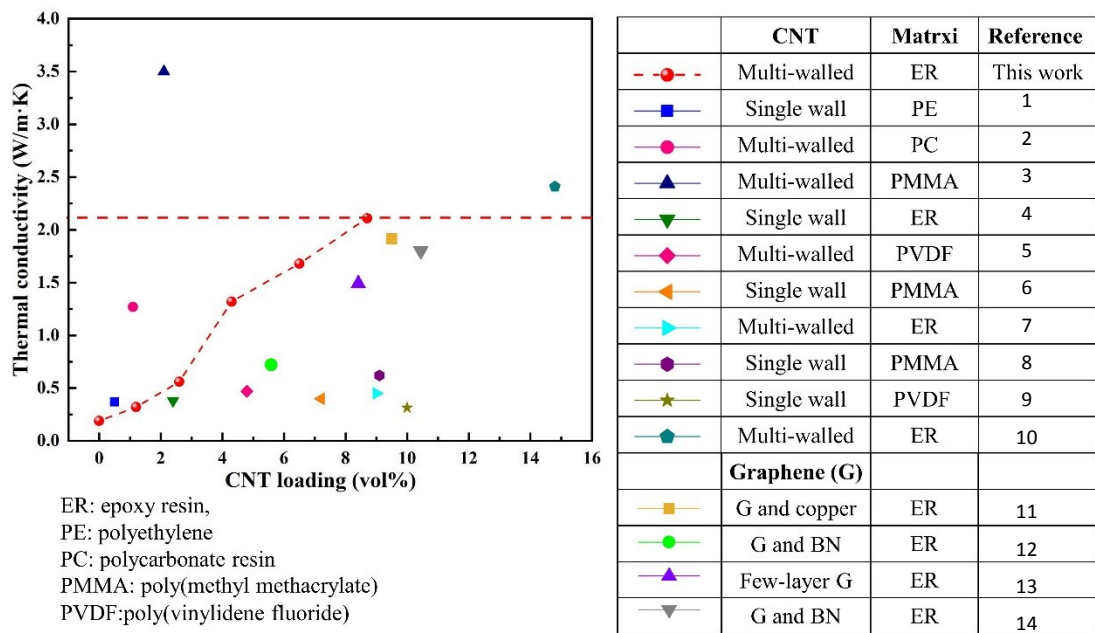


**Fig. S12** Thermal conductivity of the ER/Co@Co<sub>3</sub>O<sub>4</sub>-G nanocomposites with different loading and other CNT and graphene-based composites reported in previous work.

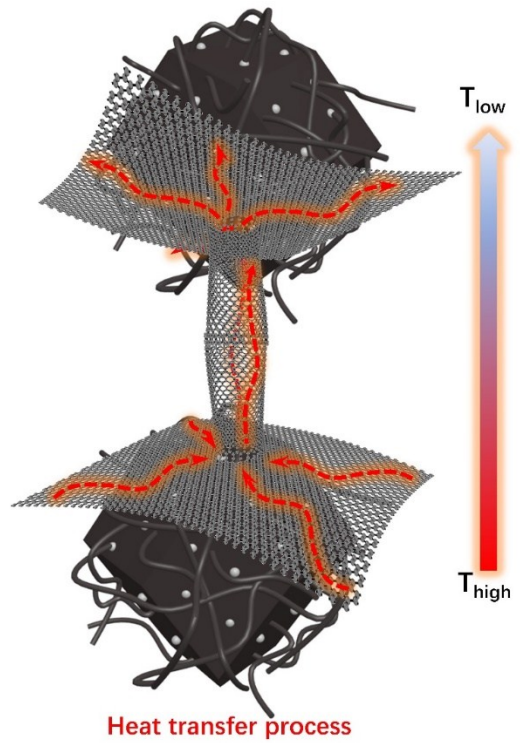


**Fig. S13** The thermal conductive mechanism of Co@Co<sub>3</sub>O<sub>4</sub>-G.

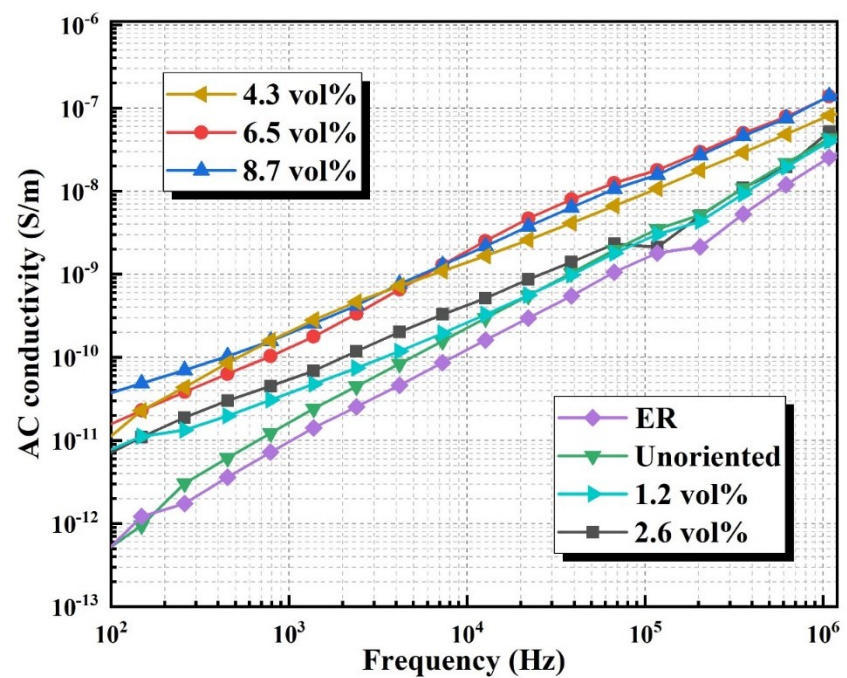


**Fig. S14** Frequency dependence of electric conductivity of the nanocomposites with different loading.

## Reference

1. R. Haggenmueller, C. Guthy, J. R. Lukes, J. E. Fischer and K. I. Winey, *macromolecules*, 2007, **40**, 2417-2424.
2. H. S. Kim, J. U. Jang, J. Yu and S. Y. Kim, *Compos. Part B-Eng.*, 2015, **79**, 505-512.
3. W. T. Hong and N. H. Tai, *Diam. Relat. Mater.*, 2008, **17**, 1577-1581.
4. F. Du, C. Guthy, T. Kashiwagi, J. E. Fischer and K. I. Winey, *J. Polym. Sci. Pol. Phys.*, 2006, **44**, 1513-1519.
5. W. B. Zhang, Z. X. Zhang, J. H. Yang, T. Huang, N. Zhang, X. T. Zheng, Y. Wang and Z. W. Zhou, *Carbon*, 2015, **90**, 242-254.
6. P. Bonnet, D. Sireude, B. Garnier and O. Chauvet, *Appl. Phys. Lett.*, 2007, **91**, 201910.
7. F. H. Gojny, M. H. G. Wichmann, B. Fiedler, I. A. Kinloch, W. Bauhofer, A. H. Windle and K. Schulte, *Polymer*, 2006, **47**, 2036-2045.
8. C. Guthy, F. Du, S. Brand, K. I. Winey and J. E. Fischer, *J. Heat Transfer*, 2007, **129**, 1096-1099.
9. Y. Xu, G. Ray and B. Abdel-Magid, *Compos. Part A-Appl. S.*, 2006, **37**, 114-121.
10. A. M. Marconnet, N. Yamamoto, M. A. Panzer, B. L. Wardle and K. E. Goodson, *ACS Nano*, 2011, **5**, 4818-4825.
11. Z. Barani, A. Mohammadzadeh, A. Geremew, C. Y. Huang, D. Coleman, L. Mangolini, F. Kargar and A. A. Balandin, *Adv. Funct. Mater.*, 2019, 1904008.
12. F. Kargar, Z. Barani, R. Salgado, B. Debnath, J. S. Lewis, E. Aytan, R. K. Lake and A. A. Balandin, *ACS Appl. Mater. Inter.*, 2018, **10**, 37555-37565.
13. F. Kargar, Z. Barani, M. Balinskiy, A. S. Magana, J. S. Lewis and A. A. Balandin, *Adv. Electron. Mater.*, 2019, **5**, 1800558.
14. J. S. Lewis, Z. Barani, A. S. Magana, F. Kargar and A. A. Balandin, *Mater. Res. Express*, 2019, **6**, 085325.